Novel properties exhibited by films of gold nanoparticle–polythiophene blends

K. Vijaya Sarathy and K. S. Narayan*

Chemistry and Physics of Materials Unit, Jawaharlal Nehru Center for Advanced Scientific Research, Jakkur P.O., Bangalore 560 064, India

Films formed by gold nanoparticle–polyoctylthiophene blends exhibit interesting structure-related properties. Microscopy studies reveal large-scale fluorescent structures spanning 1–2 microns in length, which are modulated by the metal nanoparticle distribution. Fluorescence spectroscopy measurements of the films with different concentrations of the polymer relative to the nanoparticles show interesting changes in the polymer emission bands.

CONJUGATED polymers such as derivatives of poly-paraphenylenevinylene and polylthiophene have appreciable photoluminescence (PL) efficiency and provide a viable option as the active medium in light emitting diodes[1,2]. The formation of optical quality polymer films processed from common solvents on different substrates is a significant advantage for these polymer-based devices. Another class of materials where interesting electronic, optical and structural properties have been recently observed are metal nanoparticles[3]. The nanoparticles can be chemically stabilized by the use of alkanethiols, which render them extremely inert and enable observation of particle size-dependent features. The combination of metal nanoparticles and conducting polymers in the field of molecular electronics has been studied recently, to demonstrate concepts such as molecular bridges between metal clusters[4]. In this paper we report initial studies of complex film patterns obtained from solutions of Au nanoparticles and polyoctylthiophene (P3OT) in solvents where nanoparticle stability and polymer solubility is assured. The possibility of Au nanoparticle interacting with thiophene in the polymer, leading to conformational/structural rearrangement of the polymer chains at the phase boundaries, is probed. The two phases in the films can be easily distinguished using optical microscopy because of the contrasting fluorescent properties, but, the observable length scales are however Rayleigh limited (~ $\lambda/2$). The structure of the composites and the distribution of the nanoparticles as revealed by transmission electron microscopy (TEM) and scanning electron microscopy (SEM) are also reported.

Blends of the Au–P3OT system were first prepared starting with Au organosol. The organosol containing nanoparticles of Au were synthezised[5] by the initial transfer of 3.0 ml of a 30 mM stock solution of $HAuCl_4$ from aqueous medium to toluene medium using 0.21 g of tetra-*n*-octyl ammonium bromide. This was followed by the reduction of the complexed Au ions in toluene using 2.5 ml of 0.4 M $NaBH_4$ solution, accompanied by vigorous stirring. The resulting dark red organosol was then repeatedly washed with water to remove any traces of the reducing agent (confirmed using X-ray photoelectron spectroscopy studies). P3OT was obtained from

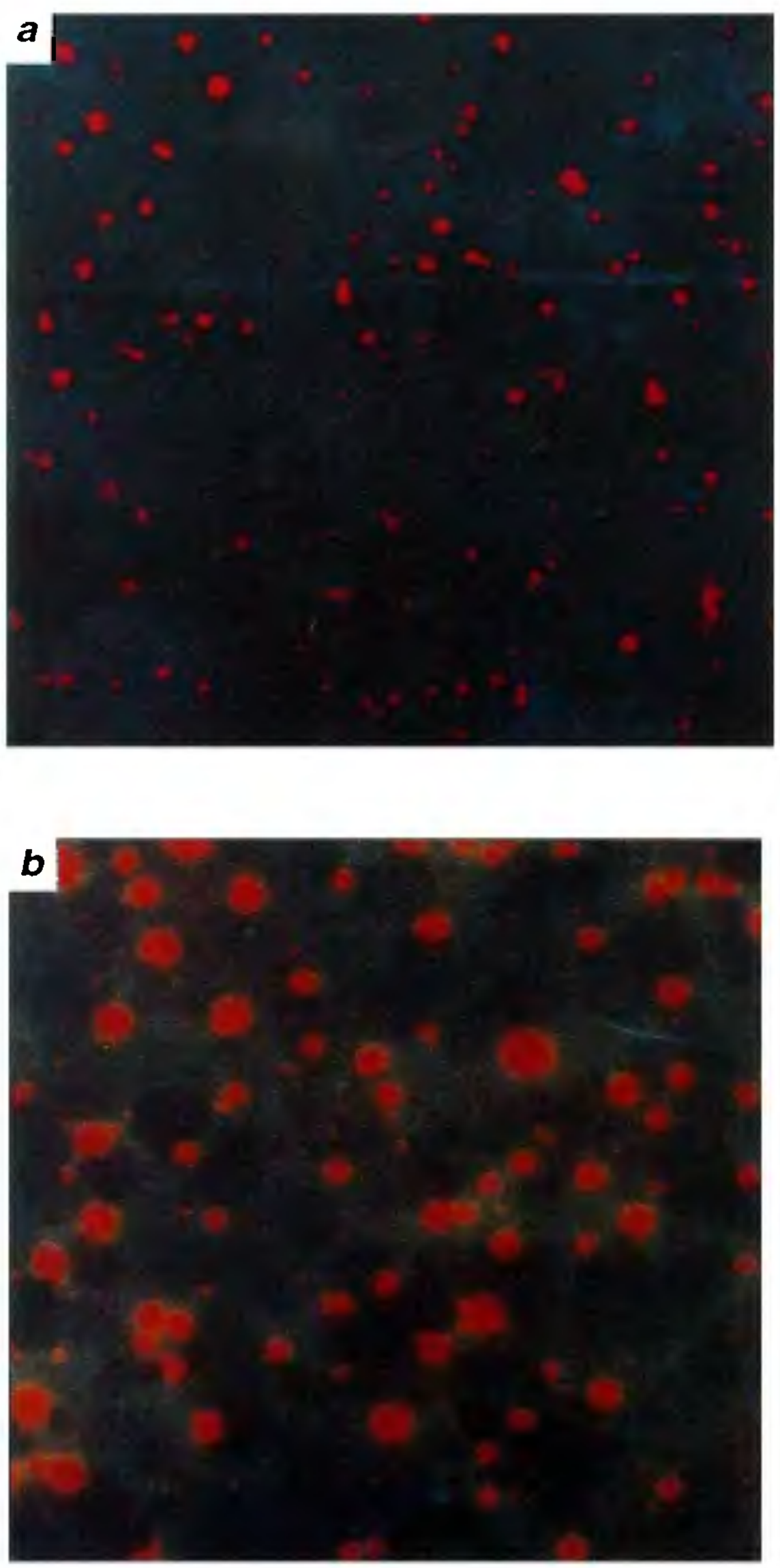

Figure 1 *a*, *b*. Optical microscope images of Au–P3OT films with two different ratios (images viewed under 400 × magnification).

*For correspondence. (e-mail: narayan@jncasr.ac.in)

Aldrich, and was dissolved in *p*-xylene in a weight–volume ratio of 2.0 mg per ml. Blends of Au–P3OT with two different ratios were obtained by the addition of polymer solution to the Au sol (0.8 ml and 1.6 ml of P3OT per ml of Au organosol). The resulting homogenous solution was stable over a period of several days with no phase separation visible due to aggregation/coagulation of the nanoparticles. In order to prepare Au nanoparticles having a lower size, the reducing agent employed was decreased to one-fifth of its initial amount in the above procedure. Blends were formed similar to the procedure followed for larger Au particles. Thin films on pre-cleaned glass substrates were deposited by spin coating and casting methods.

Optical microscopy was performed using an Olympus B2020 in epi-fluoroscence mode. A Leica S440i instrument was used for SEM studies. The histograms of the features seen in SEM studies were obtained using a Quantimet Image Analyser. TEM images were recorded with a JEOL-3010 microscope operating at 300 keV. For this purpose, the sample was prepared by placing a drop of the blend on a holey carbon grid (3 mm diameter) and subsequently evaporating it before introducing the grid into the microscope.

Large-scale morphological features were observed using optical microscopy. Randomly distributed circular features with sharp intensity contrast were present throughout the film, indicating distinct phases. The fluorescence from the circular regions was observed using different filters and different excitation wavelengths. The emission from these circular regions visually resembled the emission from a pristine polymer film which has an emission maxima centred at 680 nm (ref. 6). The size and the aural density of the circular regions are controlled by the polymer concentration with respect to gold nanoparticle as shown in Figure 1. The diameter of the fluorescing circular spots scales with the amount of the polymer concentration as evidenced by images of films with different polymer concentration in Figure 1 *a* and 1 *b*. Several other films with varying concentrations were also studied to verify this trend of increase in spot size with polymer content. The fluorescence from the spots under prolonged excitation decreases due to a bleaching process.

SEM observations provide further quantitative insight of the phase distribution with a measure of the actual sizes of the circular features. Figure 2 shows the SEM images of Au–P3OT blend where the polymer concentration is

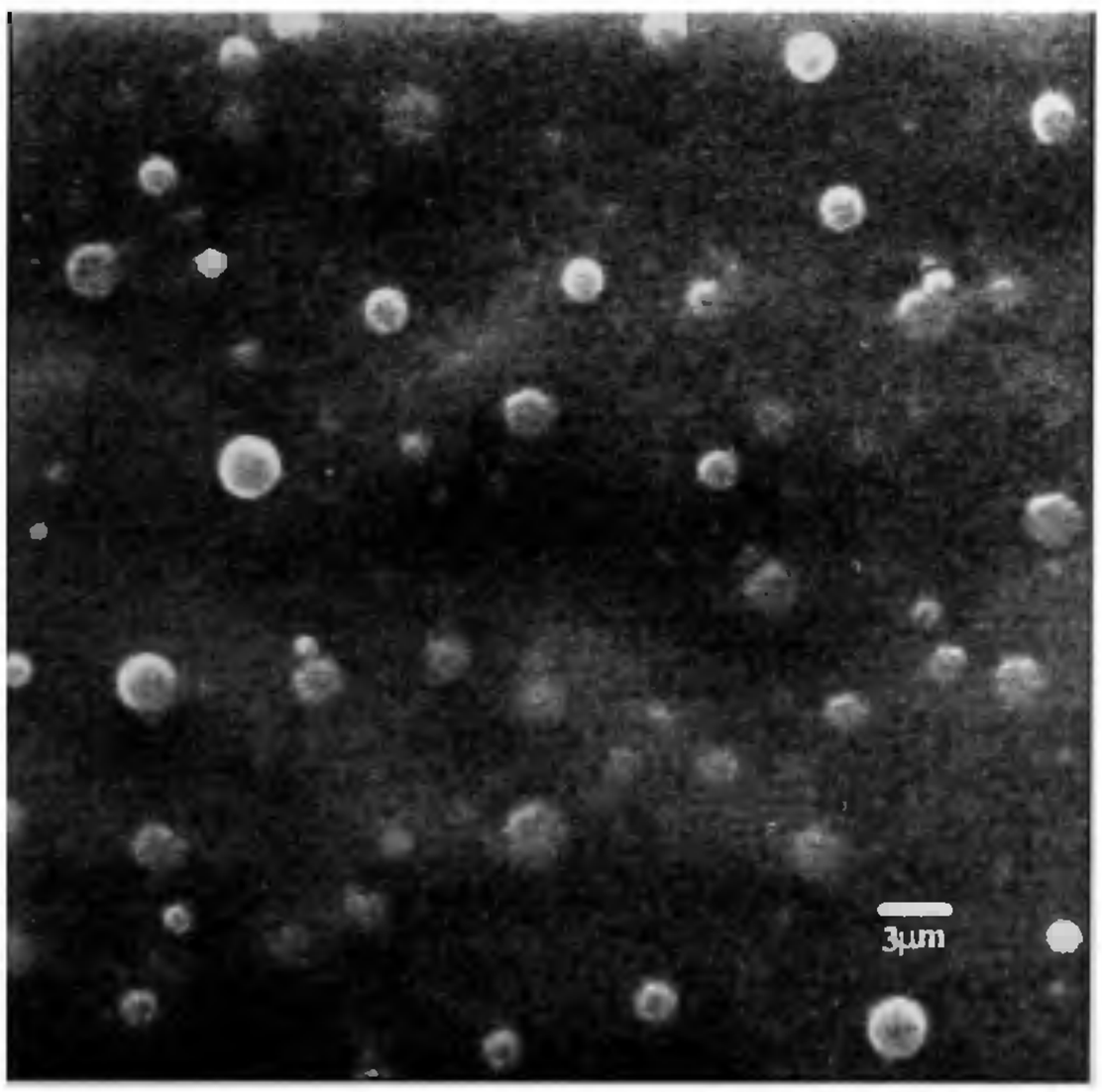

Figure 2. SEM images of Au–P3OT film showing circular features. Variation in the diameters of these features is depicted in the histogram.

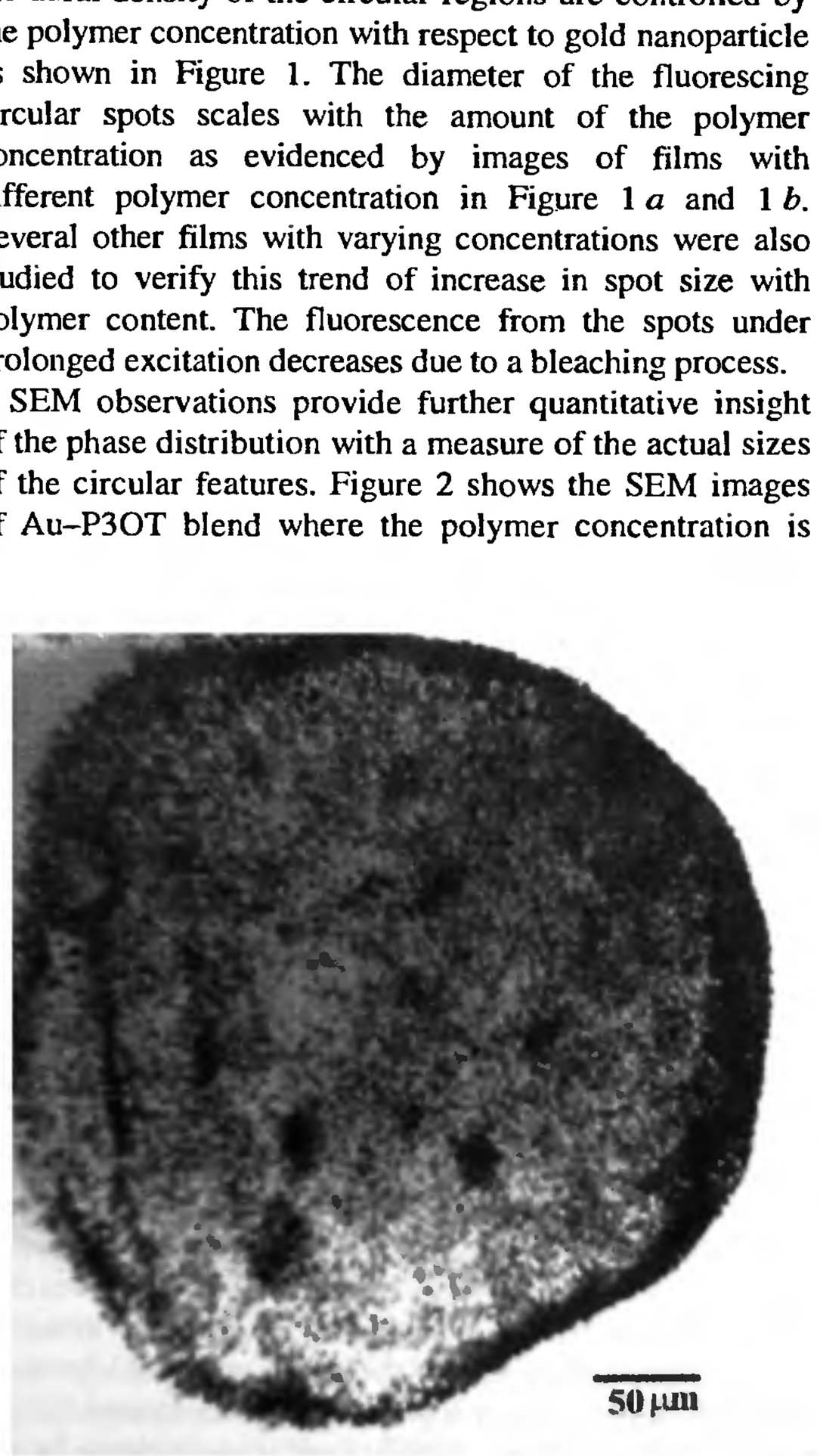

Figure 3. TEM images showing the internal morphology of the circle-like formation wherein the mean diameter of Au nanoparticles seen are ~ 7 nm.

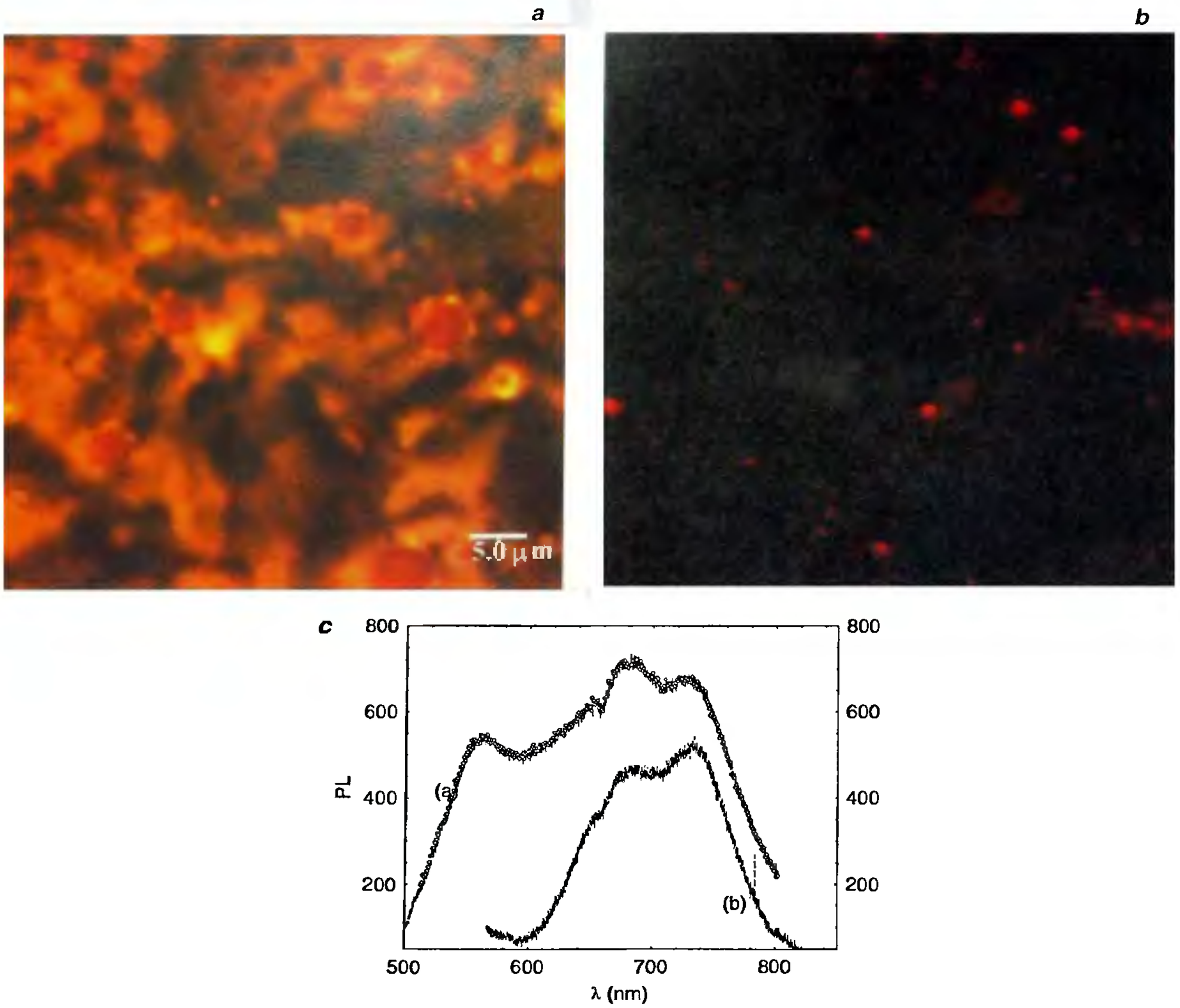

Figure 4. Confocal microscope fluorescence images of the composite films with (*a*) high and (*b*) low concentration of the polymer P3OT; *c*, typical far field PL spectra of the blends.

high. The dispersion of the circles could be a signature of the differences in the evaporation/dewetting processes of the two systems during the film formation, resulting in the creation of local domains. The average diameters of the circles are shown in Figure 2, corroborating our observations in the optical studies.

Figure 3 depicts the TEM image of a typical circular region of 0.5 μm diameter in blends with high polymer concentration. A closer observation of the TEM micrograph reveals nanoparticles with an average diameter ~ 7 nm, corresponding to the gold nanoparticle size, clustered in the circular regions. The concentration of the nanoparticles increases radially and is quite dense at the periphery, forming a ring-like structure. Rings with a hole in the centre resembling a doughnut have also been recently observed in other systems[7]. The distribution probably can be explained on the basis of competing processes in the film formation involving solvent evaporation, aggregation of the polymer chains, mobility of the nanoparticles as well as atomic level interactions between the gold and the polymer. Another feature observed in TEM studies, where the thin film of the blend is held in the holey carbon grid, is that the average sizes of the circular regions obtained were less than those observed with optical and SEM images. This feature can have its origin in the formation of films in the absence of solid substrate and which are suspended in the grid with no constraint.

Fluorescent imaging of the film was carried out using a confocal microscope (Biorad Inc.), which has improved lateral and depth resolution compared to non-confocal optical microscopy techniques. The image was recorded for the blend (particles have a mean diameter of ~ 4.0 nm

as obtained from TEM) with a high polymer concentration employing a red and a green band pass filter. The image clearly shows contribution in both the spectral regions. A real colour image constructed from these components is shown in Figure 4 *a*. The general trend is that the circular regions are primarily red with yellow contribution appearing at the periphery and outside the circular region. Another feature observed is the decrease of area with the yellow component in films with lower polymer concentration as shown in Figure 4 *b*. Far field photoluminescence spectral response of these films is consistent with the optical microscope images as shown in Figure 4 *c*. Apart from the normal PL contribution from the polymer with a $\lambda_{max} \sim 680$ nm, a distinct blue-shifted component yielding responses in the region 520 nm $< \lambda <$ 600 nm is present. The 680 nm centred emission is the expected singlet exciton radiative decay of the regioregular polymer[6]. A blue-shifted emission can arise from subtle changes in the polymer orientation, conformation or packing density due to the presence of the nanoparticles leading to changes in the electronic structure. A more direct change in the electronic density can occur if the interaction between the Au nanoparticles and the polymer interaction is appreciable, leading to charge transfer. Detailed spatially resolved fluorescence measurements are in progress along with high resolution TEM studies to probe the novel properties and unique patterns of the composite films. The fluorescence stability of the polymer in the nanoparticle environment is also being probed along with FTIR studies.

In conclusion, novel morphological and fluorescent features were observed in Au nanoparticle–P3OT composite films. The features varied with the relative concentration of the polymer with respect to the nanoparticle. The difference in the PL spectra of the blend and the pristine polymer is indicative of an interaction between the polymer and the nanoparticles.

1. Burroughs, J. H., Bradley, D. C., Brown, A. R., Marks, R. N., Mackay, K., Friend, R. H., Burn, H. and Holmes, A. B., *Nature*, 1990, **347**, 539.
2. Tessler, N., Harrison, N. T. and Friend, R. H., *Adv. Mater.*, 1998, **10**, 64.
3. Kreibig, U. and Vollmer, M., *Optical Properties of Metal Clusters*, Springer Series in Materials Science-25, 1995.
4. Brousseau III, L. C., Novak, J. P., Marinakos, S. M. and Feldheim, D. P., *Adv. Mater.*, 1999, **11**, 447.
5. Brust, M., Walker, M., Bethel, D., Schiffrin, D. J. and Whyman, R., *J. Chem. Soc., Chem. Commun.*, 1993, 96.
6. Chen, T.–A., Wu, X. and Rieke, R. D., *J. Am. Chem. Soc.*, 1995, **117**, 233.
7. Ohara, P. C., Heath, J. R. and Gelbart, W. M., *Angew. Chem., Int. Ed. Engl.*, 1997, **36**, 1077.

ACKNOWLEDGEMENTS. We acknowledge the valuable guidance of Prof. C. N. R. Rao during the entire project. We also thank Dr S. Meyer and Mr R. Sharma for confocal microscope measurements.

Received 8 July 1999; revised accepted 21 July 1999

Some aspects of presence of lead in the Delhi iron pillar

R. Balasubramaniam
Department of Materials and Metallurgical Engineering, Indian Institute of Technology, Kanpur 208 016, India

Some aspects related to the presence of lead in the Delhi iron pillar are presented in this communication. The presence of a lead solder in the joint between the decorative bell capital and the main body of the Delhi iron pillar has been confirmed by X-ray diffraction analysis of the corrosion product obtained from the joint region. The corrosion products were unambiguously identified as lead carbonate hydroxide hydrate $PbCO_3.Pb(OH)_2.H_2O$ and lead oxide carbonate Pb_2CO_4. The use of lead-based solders in joining the Delhi iron pillar's main body with the decorative bell capital is clearly established. The galvanic corrosion of iron in a lead–iron couple in soil and aqueous (3.5% NaCl solution) environments has also been studied in order to understand the nature of corrosion of the Delhi iron pillar in the buried underground regions. The corrosion of iron in soil was higher than that in the aqueous solution and the iron covered with larger area fraction of lead was corroded to a greater extent in both the environments. Severe localized corrosion of iron was observed at the defects in the lead coating. Based on the simulation experiments, it is concluded that the iron in the buried regions of the pillar is subject to severe localized corrosion due to the presence of lead coating in this region. It is recommended that the lead coating be removed and replaced with a zinc coating for the long-term preservation of the Delhi iron pillar.

THE Delhi iron pillar situated in the *Quwwat-ul-Islam* mosque complex near the Qutub Minar at New Delhi, India is widely popular for its excellent resistance to corrosion. It is a classic product of the forge welding technique used by ancient Indians to manufacture large iron objects. The material of construction of the pillar is almost pure iron with entrapped slag inclusions, which result due to the process of extraction of iron. There are several studies reported in the literature on the corrosion resistance of the pillar[1–3]. The history of the pillar[4,5], its dimensional analysis[4,6], its decorative bell capital[6] and the possible manufacturing technology employed to construct the pillar[7] have been addressed earlier. The presence of lead at several locations on the pillar has been recently addressed in detail[8] wherein visual evidences were presented. The presence of lead sheet at the bottom of the pillar is known from excavation reports[9,10]. The presence of lead appearing as black fillings between some of the iron lumps can be easily noticed on the surface of the

e-mail: bala@iitk.ac.in